

Thermoelectric effect in molecular junctions: A tool for revealing of transport mechanisms.

Dvira Segal

Department of Chemical Physics, Weizmann Institute of Science, 76100 Rehovot, Israel.

(Dated: November 11, 2018)

We investigate the thermopower of a metal-molecule-metal junction taking into account thermal effects on the junction. Based on analytical expressions and numerical simulations we show that the thermoelectric potential reveals valuable information on the mechanisms controlling the electron transfer process, including coherent transmission and thermalized hopping. We also show that at high temperatures the position of the Fermi energy relative to the molecular states can be easily deduced from the thermoelectric potential. Standard current-voltage measurements are insensitive to this information.

PACS numbers: 73.40.-c, 73.63.-b, 85.65.+h, 73.50.Lw

I. INTRODUCTION

Understanding of charge transfer processes through single molecules is at the forefront of molecular electronics [1]. The electrical conductance of a single molecule coupled to metal electrodes has been recently measured by different techniques [2, 3]. In these experiments the current-voltage (I-V) characteristic of the device is measured, and information on the transport mechanism, the molecule-metal coupling strength, and the role played by nuclear motion in the conduction process are deduced.

Experimental data [4, 5, 6] and theoretical studies [7, 8, 9, 10, 11] suggest that two mechanisms are involved in electron transfer processes through molecular bridges: Super-exchange mechanism and thermal induced hopping. The super-exchange mechanism is a coherent (tunneling) and short distance charge-transfer process. It dominates transport when the molecular levels relevant for transport- Fermi level offset is greater than the thermal energy. In the opposite limit electron transmission occurs through sequential hopping along the bridge. This is a multistep process that allows long distance charge transfer. In a typical I-V experiment transport mechanisms are analyzed based on Arrhenius plot, revealing a characteristic transition from temperature (T) independent behavior at low T to a strong dependence at high T [6].

It was recently suggested that thermoelectric measurements could provide additional insight into electron transport through *single* molecules, and contain information on the electronic and vibrational excitation spectrum of the molecule [12, 13, 14].

In a thermoelectric experiment the electric current induced by a finite temperature difference is investigated. Alternatively, the potential under the condition of zero current is measured. The thermoelectric power of microstructures such as quantum dots [15], single electron transistors, [16] and mesoscopic nanotubes [17, 18] has been of interest since it yields directly the sign of the dominant charge carriers and the intrinsic conduction properties. In addition, it is sensitive to the electronic structure at the Fermi level. In two recent studies the

thermoelectric voltage over a conjugated molecular conductor [12] and an atomic chain [13] was calculated. It yields valuable information- the location of the Fermi energy relative to the molecular levels. Inelastic interactions on the bridge were neglected in both cases. In a different work Koch *et al.* [14] investigated the thermopower of a single molecule when both sequential tunneling (lowest order tunneling process) and cotunneling (second order tunneling processes) take place. Vibrational features of the molecule were taken into account, but direct thermal activation of electrons onto the bridge and the possibility of diffusional transport were not included. In addition, this study was limited to the shortest molecular unit made of a single electronic state.

In this paper we extend these ideas and analyze the thermoelectric voltage of a molecular junction of bridge length $N > 1$ while taking into account both coherent and thermal interactions in a unified theory. Our model includes relaxation mechanisms on the bridge, arising from the interaction of the electronic system with other bridge or environmental degrees of freedom. The effect of these interactions is to open up a thermal channel for conduction. Hence in our model electrons can be transmitted through the bridge either coherently (tunneling), or by sequential hopping. We focus here on the non-resonant regime, where bridge energies are far above the chemical potentials of the metals. In this limit the actual population of electrons on the bridge is very small, and effects due to charging of the bridge (coulomb blockade) are negligible.

We show through simple approximate expressions and with numerical examples that the functional behavior of the thermoelectric voltage is intrinsically different for the different modes of transfer, and that it clearly reflects the turnover between the two mechanisms. The thermoelectric phenomena can therefore serve as a significant tool for analyzing transport mechanisms complementing traditional techniques. In addition, we find that when thermal interactions dominate the transport, the molecular levels -Fermi energy gap for transmission can be easily deduced from the thermopower value. This last property is crucial for interpreting I-V results in transport exper-

iments.

II. MODEL

The model system consists of a metal-molecule-metal junction under an electrical bias and a thermal gradient. The molecule is described by a tight binding model with N sites with one state localized at each site. The first and last states are coupled to the left (L) and right (R) metal leads respectively. At equilibrium, ϵ_F specifies the Fermi energy of the two metals, taken as the zero of energy. Under a potential bias ϕ the leads are characterized by electrochemical potentials μ_L and μ_R for the L and R sides. In addition, the two metals are kept at different temperatures T_L and T_R . For a schematic representation see Fig. 1.

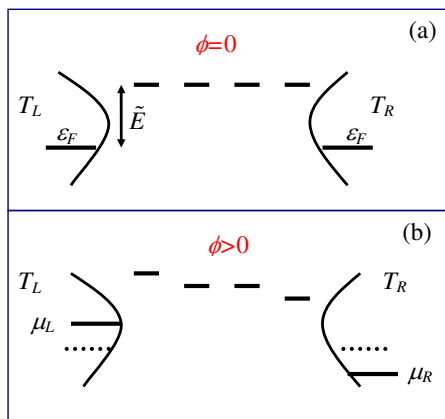


FIG. 1: (Color online) Scheme of the model system: A molecule of N sites connecting two metal leads. (a) No applied bias. (b) $e\phi > 0$.

We investigate the thermoelectric effect in this system using a variation of the model developed before to analyze thermal effects in electron transmission through molecular bridges [9, 25]. There, the molecular system and the metals were in contact with a *single* thermal reservoir held at temperature T . Here, in contrast, we specify only the temperatures of the charge reservoirs (metals), and from this boundary condition the molecular temperature should be deduced. We explain below how to implement this modification into the formalism of Ref. [9].

The system Hamiltonian includes five terms

$$H = H_M + H_K + H_{MK} + H_B + H_{MB}. \quad (1)$$

Here H_M denotes the isolated molecule of length N with one electronic state at each site

$$H_M = \sum_{j=1}^N E_j |j\rangle\langle j| + V \sum_{j=2}^N (|j\rangle\langle j-1| + |j-1\rangle\langle j|). \quad (2)$$

The bridge energies E_j are taken to be equal at all sites at zero bias, $E_j = \tilde{E}$. V is the nearest neighbors electronic

coupling. The left and right charge carriers reservoirs (metals) are described by their set of electronic states

$$H_K = \sum_{r \in R} \epsilon_r |r\rangle\langle r| + \sum_{l \in L} \epsilon_l |l\rangle\langle l|. \quad (3)$$

The leads are held at constant temperatures T_L (left) and T_R (right). In what follows we use the notations $T_a = (T_L + T_R)/2$ and $\Delta T = T_L - T_R$. The molecule-metals interaction term is

$$H_{MK} = \sum_{l \in L} V_{l,1} |l\rangle\langle 1| + \sum_{r \in R} V_{r,N} |r\rangle\langle N| + c.c. , \quad (4)$$

yielding the relaxation rate $\Gamma_L(\epsilon) = 2\pi \sum_{l \in L} |V_{l,1}|^2 \delta(\epsilon - \epsilon_l)$, and an analogous expression for Γ_R at the R side.

The molecule is in contact with thermal degrees of freedom, both internal (vibrations), and those related to the motion relative to the leads, all denoted as a "thermal bath" and included in H_B . The last term in the Hamiltonian (1) describes the coupling of this thermal bath to the molecule. Specifically we use the following model for this interaction

$$H_{MB} = \sum_{j=1}^N F_j |j\rangle\langle j|, \quad (5)$$

where F_j are bath operators and $|j\rangle$ are molecular states, $j = 1 \dots N$. The form of Eq. (5) implies that the thermal bath induces energy dephasings on the local bridge sites. The bath operators are characterized by their time correlation function

$$\int_{-\infty}^{\infty} e^{i\omega t} \langle F_j(t) F_{j'}(0) \rangle = e^{\beta\omega} \int_{-\infty}^{\infty} e^{i\omega t} \langle F_{j'}(0) F_j(t) \rangle, \quad (6)$$

where $\beta = 1/k_B T$, T is the local thermal bath temperature and k_B is the Boltzmann constant. Assuming that thermal interactions on different molecular sites are not correlated, and going into the markovian limit, the correlation function becomes

$$\langle F_j(t) F_{j'}(t') \rangle = \gamma \delta_{j,j'} \delta(t - t'). \quad (7)$$

Here γ is the dephasing rate reflecting the strength of the system-bath interaction: When $\gamma = 0$, the electronic system and the thermal degrees of freedom are decoupled, and electrons move coherently along the wire. In contrast, strong dephasing rates imply the dominance of the incoherent transmission mode [9]. It should be emphasized that the bridge dephasing rate γ and the electronic couplings between the sites V are in general temperature dependent. Since in the nonresonant regime thermal activation is the dominant temperature dependent factor, we simplify the discussion and ignore these corrections. The thermal bath temperature therefore enters the formalism only through the detailed balance condition, Eq. (6).

The transport behavior of the system depends, among other factors, on the way the potential bias falls along the

molecular bridge. In what follows we use the following model for the electrostatic potential profile

$$\begin{aligned}\mu_L &= \epsilon_F + e\phi/2; \quad \mu_R = \epsilon_F - e\phi/2; \\ E_1 &= \tilde{E} + e\phi/4; \quad E_N = \tilde{E} - e\phi/4; \\ E_j &= \tilde{E}, \quad j = 2..N-1.\end{aligned}\quad (8)$$

The qualitative aspects of the results presented below are not affected by this particular choice, since the relation $\Delta E \equiv (\tilde{E} - \epsilon_F) > e\phi$ is retained in this work.

In the weak molecule-thermal bath coupling limit a computational scheme for evaluating the energy dependent transmission coefficient through a metal-molecule-metal junction for the $T_L = T_R$ case was developed in Ref. [9]. The method is based on the generalized quantum master equations extended to steady state situations. Here we further extend this framework and study thermoelectric effects in molecular junctions.

III. THERMOPOWER

The current through the junction is calculated by generalizing the Landauer formula [19] to situations involving inelastic interactions on the bridge [20, 21]

$$\begin{aligned}I &= I_{L \rightarrow R} - I_{R \rightarrow L}, \\ I_{L \rightarrow R} &= \frac{e}{\pi\hbar} \int d\epsilon_0 \int d\epsilon_f \mathcal{T}_{L \rightarrow R}(\epsilon_0, \epsilon_f) f_L(\epsilon_0) (1 - f_R(\epsilon_f)), \\ I_{R \rightarrow L} &= \frac{e}{\pi\hbar} \int d\epsilon_0 \int d\epsilon_f \mathcal{T}_{R \rightarrow L}(\epsilon_0, \epsilon_f) f_R(\epsilon_0) (1 - f_L(\epsilon_f)).\end{aligned}\quad (9)$$

Here $\mathcal{T}_{L \rightarrow R}(\epsilon_0, \epsilon_f)$ denotes the transmission probability for an electron incoming from the left lead at the energy ϵ_0 to be emitted at the opposite side at ϵ_f . The energy difference $\epsilon_f - \epsilon_0$ is exchanged with the thermal environment. This coefficient depends on the molecular parameters, the applied potential, the metal-molecule interaction, temperature and dephasing. It is not necessarily the same for the different directions. The current (defined positive when flowing left to right) is evaluated by weighting the transmission probability by the appropriate combination of the Fermi distribution functions at the metals $f_K(\epsilon) = (e^{\beta_K(\epsilon - \mu_K)} + 1)^{-1}$ where $\beta_K \equiv (k_B T_K)^{-1}$ is the inverse temperature ($K = L, R$). Unless specified, the integrals are all taken as $\int_{-\infty}^{\infty}$.

The generalized Landauer equation does not take into account the effect of the contact population on the inelastic processes. Including such effects can be implemented by replacing the Fermi occupation factors by *nonequilibrium* electron distribution functions [7]. Yet it can be shown that Eq. (9) well approximates the current when the transmission through the junction is significantly small ($\ll 1$) [22]. Since we focus here on the out

of resonance, small bias, weak electron-phonon interaction and weak metal-molecule coupling situation, transmission probabilities are always small and Eq. (9) can be utilized. The inelastic Landauer formula can be also derived using the systematic nonequilibrium Green function approach. Recent calculations of inelastic tunneling currents yield an expression similar to (9) assuming weak coupling to the leads, weak electron-phonon coupling, and small bias [23]. For recent discussions on the issue see Refs. [14, 22, 24].

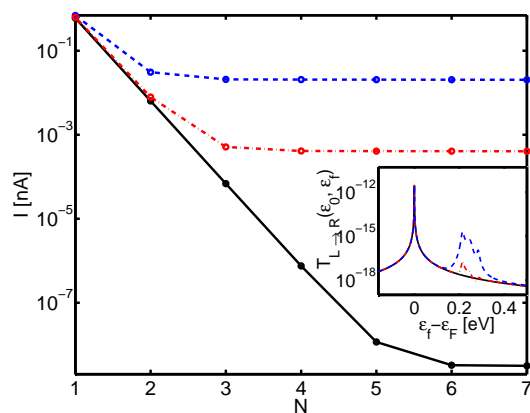


FIG. 2: (Color online) Electron current vs. wire length N for different temperatures: $T=300$ K (dashed), $T=200$ K (dashed-dotted) and $T=100$ K (full). The other parameters are $\Delta E=250$ meV, $V=25$ meV, $e\phi=2.5$ meV, $\Gamma_L = \Gamma_R=15$ meV, $\gamma=1$ meV. The inset presents the respective L to R transmission probability $\mathcal{T}_{L \rightarrow R}$ for $N=3$ and $\epsilon_0 = \epsilon_F$. $T=300$ K, 200 K, 100 K top to bottom.

We calculate next the current flowing through a biased N level molecular junction. We first consider the simple situation of $T_L = T_R = T$, i.e. we do not apply an external temperature gradient. Since this system was analyzed extensively in previous works, Refs. [9, 25], we present here only the main results. Fig. 2 demonstrates the distance dependence of the current at different temperatures. The following set of parameters is used: $\Delta E = 250$ meV, $V = 25$ meV, $e\phi = 2.5$ meV and $\gamma = 1$ meV (Typical dephasing times in condensed phases are of order of 1 ps). The inset depicts the corresponding energy resolved transmission probability for an electron incoming at $\epsilon_0 = \epsilon_F$ for the $N = 3$ case.

The following observations can be made: (i) The transmitted flux consists in general two main components: elastic tunneling at $\epsilon_f = \epsilon_0$ and activated flux in the energy range of the bridge states $\sim \Delta E$. These two components can be clearly distinguished when bridge energies are high enough, $\Delta E \gg k_B T$ and the coherent interaction V is much smaller than ΔE . (ii) The coherent component is most important at low temperatures, large energy gaps and short chains. The incoherent contribution dominates in the opposite limits. (iii) The electric current manifests a clear transition from an exponential decay typical to tunneling for short chains, to a weak (al-

gebraic) distance dependence for longer chains, characterizing thermal activation into the bridge. The turnover is shifted into higher N values when the temperature is lowered. (iv) The thermal component of the transmission is exponentially enhanced when increasing the temperature. In contrast, the effect of the dephasing is more subtle. When the dephasing rate is very small $\gamma < 0.01$ meV (using the parameters of Fig. 2), transport is coherent and the current increases with γ . For very high dephasing values, $\gamma \sim 100$ meV, coherent effects are completely destroyed and the current *goes down* like $1/\gamma$. See Ref. [9] for details. In this work we employ the intermediate values of $\gamma \sim 0.1 - 10$ meV.

Following these observations we can approximate the transmission coefficient by a generic functional form containing only its main features: For large energy gaps and for reasonable temperatures mixed coherent-inelastic contributions can be safely neglected and the transmission is approximated by two separate terms [9, 25]

$$\mathcal{T} = \mathcal{T}_{tunn} + \mathcal{T}_{hopp}. \quad (10)$$

The first term stands for tunneling

$$\mathcal{T}_{tunn}(\epsilon_0, \epsilon_f) = \delta(\epsilon_0 - \epsilon_f)A(\epsilon_0), \quad (11)$$

while the second contribution reproduces thermalized hopping through the junction

$$\mathcal{T}_{hopp}(\epsilon_0, \epsilon_f) = B(\epsilon_0, \epsilon_f)e^{-\beta(E_B - \epsilon_0)}. \quad (12)$$

E_B is an effective bridge energy. It is related closely to the gap ΔE of the molecule in an equilibrium situation, but it is modified by the molecule-metal interactions and the applied potential. The coefficients A and B depend on the molecule-metal coupling terms, the energetics of the bridge, its length, and on the thermal parameters T and γ . Here we assume that A does not depend on the thermal parameters, and that B is the same when exchanging between the initial and final energies, $B(\epsilon_0, \epsilon_f) = B(\epsilon_f, \epsilon_0)$ [9]. In what follows we utilize Eqs. (11)-(12) for deriving simple expressions for the thermopower coefficient.

We proceed to the relevant case of an electrically biased junction under an additional temperature gradient. In our model the temperatures of the two leads L and R are kept fixed at T_L and T_R respectively, while the temperature of the molecular degrees of freedom is adjusted to the boundary conditions: At a steady state situation the temperature distribution along the molecule is determined, among other factors, by the metals temperatures, the rate of energy dissipation on the molecule, and the rate at which energy is transferred away from the conductor [25, 26]. Here we do not calculate this temperature gradient, but assume that at the left end of the molecular chain the temperature is nearly T_L , and similarly at the right edge it is close to T_R .

We assume next that the transmission $\mathcal{T}_{K \rightarrow K'}$ depends on the temperature T_K ($K=L,R$), but is independent of

$T_{K'}$. Under this approximation the transmission coefficient in Eq. (9) can be calculated using the procedure of Refs. [9, 25] without modifications, simply by employing the different temperatures when evaluating $\mathcal{T}_{L \rightarrow R}$ and $\mathcal{T}_{R \rightarrow L}$. This approximation relies on the fact that in the $K \rightarrow K'$ transmission process the temperature at the K end dominates the transport. This is true considering both transport mechanisms, tunneling and sequential hopping: Hopping through the bridge is triggered by thermal activation from the metal, see Eq. (12). Assuming that this is the rate determining step, the relevant temperature is therefore T_K . The tunneling contribution to transmission depends very weakly on the bridge's temperature [9]. This naive approximation is adjusted by maintaining $\Delta T \rightarrow 0$. Note that a full self consistent formalism (For example the Keldish-Kadanoff formalism [27]) should naturally yield the temperature distribution on the junction without such assumptions.

We define the thermoelectric voltage $\phi|_{I=0}$ as the voltage necessary for neutralizing the temperature induced current. The thermopower is the ratio of the potential energy $e\phi$ to the temperature difference ΔT under the condition that the current vanishes

$$S = - \lim_{\Delta T \rightarrow 0} \left. \frac{e\phi}{k_B \Delta T} \right|_{I=0}. \quad (13)$$

We discuss next the limiting behavior of the thermopower ratio for the different transport mechanisms. The net current is calculated by considering separately the elastic (tunneling) and inelastic (hopping) components, Eqs. (10)-(12). The tunneling current reduces to the standard Landauer formula [19]

$$I_{tunn} = \frac{e}{\pi \hbar} \int d\epsilon_0 A(\epsilon_0) [f_L(\epsilon_0) - f_R(\epsilon_0)]. \quad (14)$$

Assuming the transmission is a smooth function of the energy in comparison to $k_B T_a$, it can be expanded around ϵ_F

$$\begin{aligned} A(\epsilon) &= A(\epsilon_F) + \left. \frac{\partial A}{\partial \epsilon} \right|_{\epsilon_F} (\epsilon - \epsilon_F) + \frac{1}{2!} \left. \frac{\partial^2 A}{\partial \epsilon^2} \right|_{\epsilon_F} (\epsilon - \epsilon_F)^2 \\ &+ \frac{1}{3!} \left. \frac{\partial^3 A}{\partial \epsilon^3} \right|_{\epsilon_F} (\epsilon - \epsilon_F)^3 + \dots \end{aligned} \quad (15)$$

In the linear response regime of small ΔT and ϕ the Fermi functions in Eq. (14) are further expanded linearly

$$f_L(\epsilon) - f_R(\epsilon) = - \frac{\partial f(\epsilon, \epsilon_F, T_a)}{\partial \epsilon} \left[e\phi + \frac{\Delta T}{T_a} (\epsilon - \epsilon_F) \right]. \quad (16)$$

Here the derivative of the Fermi function is calculated at the average values T_a and ϵ_F . When we consider only the first two terms in Eq. (15) in conjunction with Eq. (16), we obtain the standard lowest order expression for electron current due to both electric bias and temperature gradient [12, 13, 28]

$$I_{tunn} = - \frac{e^2}{\pi \hbar} A(\epsilon_F) \phi + \frac{e}{\pi \hbar} \frac{\pi^2 k_B^2 T_a}{3} \left. \frac{\partial A}{\partial \epsilon} \right|_{\epsilon_F} \Delta T. \quad (17)$$

The current through the device is zero when the potential difference is set to

$$\phi|_{I=0} = \frac{\pi^2 k_B^2 T_a}{3e} \left. \frac{\partial(\ln(A))}{\partial \epsilon} \right|_{\epsilon=\epsilon_F} \Delta T. \quad (18)$$

When higher order terms in A are necessary, we utilize the Sommerfeld expansion [29] and get a power law series in T_a for the thermoelectric potential

$$\phi|_{I=0} \sim \frac{k_B \Delta T}{e A(\epsilon_F)} \left(\sum_{n=1,3,5,\dots} \left. \frac{\partial^n A}{\partial \epsilon^n} \right|_{\epsilon_F} (k_B T_a)^n \right). \quad (19)$$

We can further consider an explicit expression for A . If the bridge energies lies well above μ_L and μ_R , a perturbative treatment leads to the superexchange result [30]

$$A(\epsilon_0) \sim \frac{V^{2N}}{(E_B - \epsilon_0)^{2N}} \Gamma. \quad (20)$$

Here V is the coupling matrix element in the bridge and $\Gamma = \Gamma_K$ is the relaxation rate to the K metal. We substitute this relation into Eq. (19) and get the tunneling contribution to the thermopower

$$-\frac{e\phi|_{I=0}}{k_B \Delta T} \sim \sum_{n=1,3,5,\dots} (2N)^n \frac{(k_B T_a)^n}{(E_B - \epsilon_F)^n} \equiv S_T. \quad (21)$$

This expression, though approximate, provides us with the important features of S_T : the *inverse* dependence with energy gap, and its enhancement with size and temperature.

When the gap ($E_B - \epsilon_F$) is large and the bridge size N is long such that A is practically zero away from the bridge energies, i.e. $A(\epsilon) \propto \delta(\epsilon - E_B)$, the tunneling contribution from ϵ_F approaches zero. Electron transmission occurs then mainly via electrons in the tails of the Fermi distributions in the leads at energies around E_B . In this ballistic regime the current, Eq. (14), is zero when $f_L(E_B) = f_R(E_B)$ or

$$\beta_L(E_B - \mu_L) = \beta_R(E_B - \mu_R). \quad (22)$$

Using $T_L = T_a + \Delta T/2$, $T_R = T_a - \Delta T/2$, $\mu_L = \epsilon_F + e\phi/2$ and $\mu_R = \epsilon_F - e\phi/2$, it reduces to

$$-\frac{e\phi|_{I=0}}{k_B \Delta T} = \frac{E_B - \epsilon_F}{k_B T_a} \equiv S_B. \quad (23)$$

This is the thermopower ratio in the ballistic regime: Electrons physically populate the molecule, but inelastic effects on the bridge are neglected. The thermopower in this case scales like T_a^{-1} , in accordance with previous studies [14].

Next we estimate the thermopower when thermal interactions govern the transport across the bridge. We substitute Eq. (12) into Eq. (9) using $\beta = \beta_K$ for the

$\mathcal{T}_{K \rightarrow K'}$ calculation, and get the net thermal (hopping) current

$$I_{hopp} = \frac{e}{\pi \hbar} \int d\epsilon_f \int d\epsilon_0 B(\epsilon_0, \epsilon_f) (1 - f_L(\epsilon_0))(1 - f_R(\epsilon_f)) \times \left[e^{-\beta_L(E_B - \mu_L)} - e^{-\beta_R(E_B - \mu_R)} \right]. \quad (24)$$

It is zero when the term in the square parentheses vanishes, i.e.

$$\beta_L(E_B - \mu_L) = \beta_R(E_B - \mu_R), \quad (25)$$

which leads to

$$-\frac{e\phi|_{I=0}}{k_B \Delta T} = \frac{E_B - \epsilon_F}{k_B T_a} \equiv S_H. \quad (26)$$

This result is equivalent to Eq. (23). There we considered resonant-coherent-transmission through a long chain, when tunneling from the Fermi energy is negligible. Therefore, we cannot distinguish in the thermopower between transport due to thermal activation from the lead to the molecule and band motion of electrons at the tails of the Fermi function. We refer to both as thermal mechanisms.

We compare next the tunneling thermopower term S_T , Eq. (21), to the thermalized behavior S_H , (Eqs. (23), (26)). The following observations can be made: (i) $S_T \sim (T_a/\Delta E)^n$, while $S_H \sim \Delta E/T_a$. Here $\Delta E \equiv E_B - \epsilon_F$. (ii) The tunneling term depends on the length of the molecule N . (iii) In both cases S does not depend on the molecule-metal interaction strength, given by the parameter Γ . (iv) Measurement of S vs. T_a should yield the effective energy gap for transmission, and also hint on the transport mechanism. We expect that when increasing the temperature, the thermopower should first increase (tunneling behavior governs at low temperatures), then decay in a T_a^{-1} fashion when thermal activation dominates electron transfer.

IV. RESULTS

We investigate the thermopower behavior in our model system, Eqs. (1)-(8), and show how the approximate expressions, Eqs. (21) and (26), agree well with the numerical results. We also extract important energetic and dynamic information from the thermoelectric potential. The following set of parameters is used: $N \sim 1-5$ units, molecular energies $\tilde{E} \sim 100-500$ meV (ϵ_F is taken as zero). We focus on the limit $\tilde{E} > V$ using $V=25$ meV. The metal-molecule relaxation rate is taken equal at the L and R sides, $\Gamma_K = 15$ meV. The system bath interaction is given by the dephasing parameter, $\gamma \sim 0.5 - 10$ meV.

Fig. 3 shows the I-V characteristic for a chain of size $N=4$ for different energy gaps \tilde{E} using $T_L=335$ K and $T_R=300$ K. Within this set of parameters the current is dominated by thermal effects, see Fig. 2. Note that the

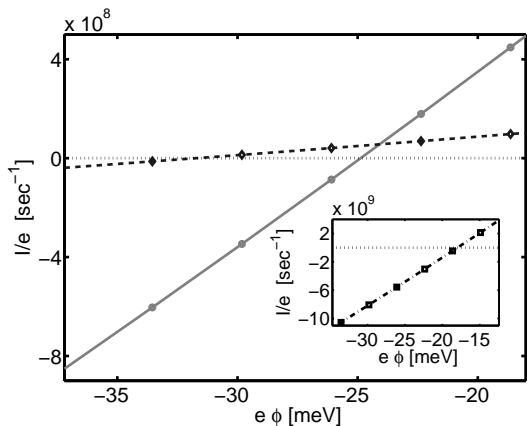


FIG. 3: I-V characteristics of the $N=4$ junction. The system parameters are $\gamma=5$ meV, $T_L=335$ K, $T_R=300$ K. $\tilde{E} = 315$ meV (dashed), $\tilde{E} = 250$ meV (full). The dotted line shows for reference the $I=0$ function. Inset: $\tilde{E} = 185$ meV.

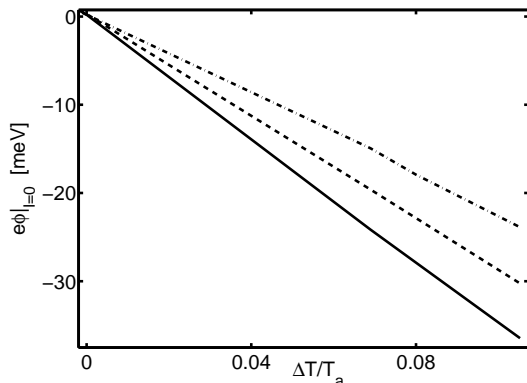


FIG. 4: The thermoelectric voltage plotted against $\Delta T/T_a$ for different metal-molecule energy gaps. $\tilde{E}=375$ meV (full), $\tilde{E}=315$ meV (dashed), and $\tilde{E}=250$ meV (dashed-dotted). $N=4$, $\gamma=5$ meV, $\Delta T=30$ K.

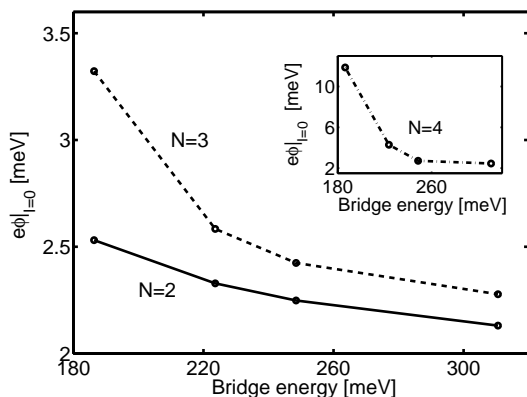


FIG. 5: Dependence of the thermoelectric voltage on the bridge energy (\tilde{E}) in the superexchange regime. $\gamma=0.5$ meV, $T_a=100$ K, $\Delta T=-20$ K. $N=2$ (full), $N=3$ (dashed). Inset: $N=4$.

I-V characteristic is expected to be linear for $e\phi < k_B T_K$ for both coherent and incoherent modes of transfer [25]. This property enables easy and accurate evaluation of the $\phi|_{I=0}$ value by a linear fitting of a few I-V data points.

We find that the results perfectly agree with Eq. (26). For $\tilde{E}=315$ meV (dashed) the current vanishes at $e\phi|_{I=0}=-32$ meV. When utilizing Eq. (26) this number provides an effective energy gap of $E_B=290$ meV. This value is in agreement with the lowest diagonalized bridge energy of $\sim \tilde{E} - V=315-25=290$ meV. The same behavior is obtained for $\tilde{E}=250$ meV (full) where we get $e\phi|_{I=0}=-25$ meV, leading to $E_B=227$ meV. For $\tilde{E}=187$ meV (inset) the zero-current voltage is $e\phi|_{I=0}=-18$ meV and the resulting gap is $E_B=163$ meV. We note that the effective energy gap E_B calculated (or measured) based on the thermoelectric effect is the *real* gap in the system, taking into account naturally and consistently the metal-molecule interaction, the thermal effects and the applied bias.

Fig. 4 demonstrates the temperature dependence of the thermoelectric voltage within the same range of parameters. It provides another evidence that in the present case transport is dominated by thermal activation as $\phi|_{I=0} \propto \Delta T/T_a$, in agreement with Eq. (26). The slopes for the $\tilde{E} = 375, 315, 250$ meV cases are 316, 267, 217 meV respectively, producing the effective gaps. Note that for different thermoelectric voltages the bridge energies are slightly varied according to Eq. (8). For accurate results measurements should be done at $\Delta T \rightarrow 0$.

We turn now to the low temperature regime where tunneling is expected to dominate charge transfer. Fig. 5 presents the potential $\phi|_{I=0}$ for various chain lengths as a function of the energy gap \tilde{E} using $T_a=100$ K and $\gamma=0.5$ meV. Indeed we find that the thermoelectric voltage *decreases* with increasing gap in contrast to its behavior (in absolute values) in figures 3 and 4. In addition, the thermoelectric voltage is larger for longer bridges. These observations are consistent with Eq. (21).

Next we show that the temperature induced turnover between coherent motion to incoherent transmission is reflected in the thermoelectric potential. Fig. 6 exemplifies this behavior. We observe mainly three regimes in the main curve: (a) The potential is almost zero. (b) $e\phi|_{I=0}$ increases strongly with T_a . (c) Above the threshold of $T_a \sim 150$ K the potential saturates, then goes down like $\propto \Delta T/T_a$. We can explain these results as follows: (a) At very low temperatures the thermoelectric potential is close to zero as tunneling transmission through the bridge is very small. Ballistic motion is not significant because of the low population of electrons at the metals around E_B . (b) When the temperature is increased electrons populate energies in the metals above the Fermi energy and tunneling becomes more probable. Band motion and thermalized hopping also begin to contribute. (c) In this regime transport occurs through physical population of the bridge, and the thermopower behaves in accordance with Eq. (26). To conclude- while in region (a) transport is dominated by coherent interac-

tions, in region (c) it is induced by thermal effects. The intermediate area (b) presents a regime where coherent effects and thermal interactions mix. The inset displays the Arrhenius plot of $\ln(I)$ vs. inverse temperature for a representative applied potential, $e\phi = 6$ meV (The results do not depend on the applied voltage for $e\phi$ up to ~ 30 meV). The different regimes are marked according to the main plot. A clear transition at $T_a \sim 100$ K is observed: The current becomes temperature independent for lower temperatures since tunneling dominates. The behavior at region (c) is also clear: $\ln(I) \propto 1/T_a$. In contrast, the behavior at the central area is obscure, and no clear transition is observed at $T_a \sim 150$ K. Thus, thermopower measurements may complement standard I-V studies, yielding valuable information about the junction energetics and charge transfer mechanisms.

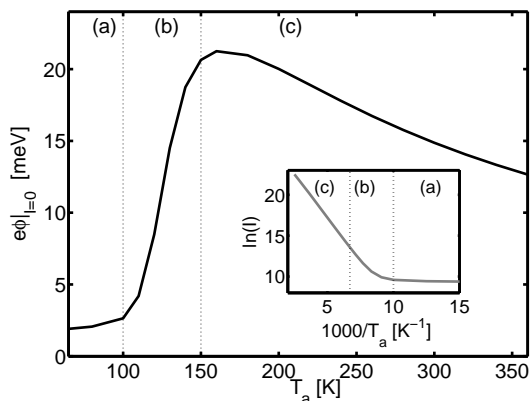


FIG. 6: Temperature dependence of the thermoelectric voltage. $\tilde{E}=250$ meV, $N = 4$, $\gamma=1$ meV, $\Delta T= -20$ K. Inset: Arrhenius plot of current vs. inverse temperature for $e\phi = 6$ meV.

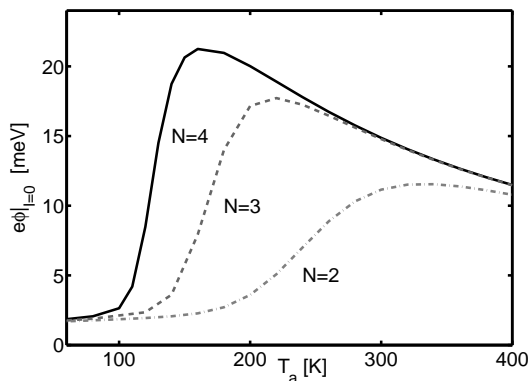


FIG. 7: Temperature dependence of the thermoelectric voltage for different bridge lengths. $N=4$ (full), $N=3$ (dashed), $N=2$ (dashed-dotted). $\tilde{E}=250$ meV, $\gamma=1$ meV, $\Delta T= -20$ K.

Finally, Fig. 7 displays the thermoelectric potential vs. temperature for molecules of different sizes: $N=4$ (full), $N=3$ (dashed), and $N=2$ (dashed-dotted). We find that for short chains the transition points between the three regimes are shifted to higher temperatures as coherent effects persist. For the $N=2$ chain transport is still largely controlled by tunneling at room temperature. Another important feature of the thermoelectric potential is its independence on N at high temperatures, while it is strongly size dependent at low T_a . This observation is consistent with expressions (21) and (26).

V. SUMMARY

Using a simple model for electron transfer through a molecular junction, taking into account both coherent effects and thermal interactions in the molecule, we have calculated the thermopower of the device assuming weak molecule-leads and weak molecule-thermal baths interactions. We have shown that the thermopower can provide information on charge transfer mechanisms, and that it can reveal the location of the Fermi energy relative to the molecular levels. Thermopower measurements can thus complement standard I-V experiments, with the advantage of their insensitivity to the metal-molecule contact. For example, the thermopower can be used for comparing of transport experiments done on the same molecules but with different contact interactions and measurement methods [31].

Acknowledgments

The author would like to thank A. Nitzan and M. Shapiro for useful comments. This research was supported by a grant from the Feinberg graduate school of the Weizmann Institute of Science.

- [1] A. Nitzan, M. A. Ratner, *Science* **300**, 1384 (2003).
- [2] S. J. Tans *et al.*, *Nature* **386**, 474 (1997).
- [3] R. H. M. Smit *et al.*, *Nature* **419**, 906 (2002).
- [4] W. B. Davis, W. A. Svec, M. A. Ratner, M. R. Wasielewski, *Nature* **396**, 60 (1998).

- [5] B. Giese, J. Amaudrut, A.-K. Köhler, M. Spormann, S. Wessely, *Nature* **412**, 318 (2001).
- [6] Y. Selzer, M. A. Cabassi, T. S. Mayer, D. L. Allara, J. Am. Chem. Soc. **126**, 4052 (2004); *Nanotechnology* **15**, S483 (2004).

- [7] E. G. Emberly, G. Kirczenow, Phys. Rev. B **61**, 5740 (2000).
- [8] H. Ness, S. A. Shevlin, A. J. Fisher, Phys. Rev. B **63**, 125422 (2001); H. Ness, A. J. Fisher, Phys. Rev. Lett. **83**, 452 (1999).
- [9] D. Segal, A. Nitzan, W. B. Davis, M. R. Wasielewski, M. A. Ratner, J. Phys. Chem. B **104**, 3817 (2000); D. Segal, A. Nitzan, M. A. Ratner, W. B. Davis, J. Phys. Chem. **104**, 2790 (2000); D. Segal, A. Nitzan, Chem. Phys. **268**, 315 (2001); **281**, 235 (2002).
- [10] M. J. Montgomery, J. Hoekstra, T. N. Todorov, A. P. Sutton, J. Phys.: Condens. Matter **15**, 731 (2003).
- [11] E. G. Petrov, V. May, J. Phys. Chem. A **105**, 10176 (2001). E. G. Petrov, Y. R. Zelinsky, V. May, J. Phys. Chem. B **106**, 3092 (2002); E. G. Petrov, V. May, P. Hänggi, Chem. Phys. **296**, 251 (2004).
- [12] M. Paulsson, S. Datta, Phys. Rev. B **67**, 241403 (2003).
- [13] X. Zheng, W. Zheng, Y. Wei, Z. Zeng, J. Wang, J. Chem. Phys. **121**, 8537 (2004).
- [14] J. Koch, F. Von Oppen, Y. Oreg, E. Sela, Phys. Rev. B **70**, 195107 (2004).
- [15] C. W. J. Beenakker, A. A. M. Staring, Phys. Rev. B **46**, 9667 (1992).
- [16] K. A. Matveev, A. V. Andreev, Phys. Rev. B **66**, 045301 (2002).
- [17] J. Hone *et al.*, Phys. Rev. Lett. **80**, 1042 (1998).
- [18] J. P. Small, K. M. Perez, P. Kim, Phys. Rev. Lett. **91**, 256801 (2003).
- [19] R. Landauer, Philos. Mag. **21**, 863 (1970); R. Landauer, IBM J. Res. Dev. **1**, 223 (1957).
- [20] K. Haule, J. Bonča, Phys. Rev. B **59**, 13087 (1999).
- [21] A. Nitzan, Annu. Rev. Phys. Chem. **52**, 681 (2001).
- [22] V. B. Antonyuk, A. G. Mal'shukov, M. Larsson, K. A. Chao, Phys. Rev. B **69**, 155308 (2004).
- [23] M. Galperin, A. Nitzan, M. A. Ratner, D. R. Stewart, J. Phys. Chem. B **109**, 8519 (2005).
- [24] M. Čížek, M. Thoss, W. Domcke, Phys. Rev. B **70**, 125406 (2004).
- [25] D. Segal, A. Nitzan, J. Chem. Phys. **117**, 3915 (2002).
- [26] D. Segal, A. Nitzan, P. Hänggi, J. Chem. Phys. **119**, 6840 (2003).
- [27] L. P. Kadanoff and G. Baym, Quantum Statistical Mechanics. (Benjamin-Cummings, Reading, MA, 1962); L. V. Keldysh, Sov. Phys. JETP **20**, 1018 (1965).
- [28] C. R. Proetto, Phys. Rev. B **44**, 9096 (1991).
- [29] N. W. Ashcroft, N. D. Mermin, Solid State Physics (Saunders College publishing, Philadelphia 1976).
- [30] H. M. McConnell, J. Chem. Phys. **35**, 508 (1961).
- [31] A. Salomon *et al.*, Advanced Materials **15**, 1881 (2003).